Influence of Crystal Structure on the Tableting Properties of Sulfamerazine Polymorphs

Changquan Sun[1,2] and David J. W. Grant[1,3]

Received October 15, 2000; accepted November 14, 2000

Purpose. To understand the influence of polymorphic structure on the tableting properties of sulfamerazine.

Methods. Bulk powders of sulfamerazine polymorph **I** and of two batches, **II(A)** and **II(B)** of different particle size, of polymorph **II** were crystallized. The powders were compressed to form tablets whose porosity and tensile strength were measured. The relationships between tensile strength, porosity and compaction pressure were analyzed by the method developed by Joiris, E., et al. *Pharm. Res.* **15**:1122–1130 (1998).

Results. The sensitivity of tensile strength to compaction pressure, known as the tabletability, follows the order, **I** >> **II(A)** > **II(B)** and the porosity at the same compaction pressure, which measures the compressibility, follows the order, **I** << **II(A)** < **II(B)**. Therefore, the superior tabletability of **I** over **II(A)** or **II(B)** is attributed to its greater compressibility. Molecular simulation reveals slip planes in crystals of **I** but not in **II**. Slip planes provide **I** crystals greater plasticity and therefore greater compressibility and tabletability. Larger crystal size of **II(B)** than of **II(A)** leads to fewer contact points between crystals in the tablets and results in a slightly lower tabletability.

Conclusions. Slip planes confer greater plasticity to crystals of **I** than **II** and therefore greater tabletability.

KEY WORDS: plasticity; porosity; slip planes; sulfamerazine polymorphs; tabletability; tensile strength.

INTRODUCTION

Many pharmaceutical solids exhibit polymorphism, i.e., the ability of a substance to exist as two or more crystalline phases that have different arrangements and/or conformations of the molecules in the crystal lattice (1). Because of their structural differences, polymorphs may have different solid-state properties, e.g., density, habit, color, refractive index, melting properties, solubility, dissolution rate, hydrogroscopicity, and mechanical properties (1). Consequently, polymorphism can exert profound effects on pharmaceutical processing, e.g., milling, granulation, and tableting (2–6).

For example, polymorph B of phenylbutazone is more ductile and tends to form stronger bonding than polymorph A (5). However, the deformation of polymorph B is more sensitive to compression rate (5). For chlorpromazine hydrochloride, different polymorphs may be formed in granules when using different solvents for wet granulation. The changes in the crystal form produced by wet granulation result in different bonding properties of this drug (6). For carbochromen hydrochloride, Form II′ crystals take up water more easily than Form I′ and convert to the dihydrate. Consequently, cracking of tablets of Form II′ was observed during storage, while tablets of Form I′ did not crack under the same storage conditions (7). Carbamazepine granules may contain different polymorphs depending on the binder solution that is used during wet granulation. Powders with different polymorphic contents of carbamazepine, when compressed under the same conditions, lead to tablets of different hardness (3). These studies clearly indicate that polymorphism influences the tableting behavior of pharmaceuticals, but did not provide a fundamental understanding to the observations. Therefore, little predictive capability of the effects of polymorphism on tableting properties can be deduced from the above mentioned results.

A recent fundamental study has shown that the different yield strengths of two polymorphs of acetaminophen are related to their crystal structures (8). A molecular simulation approach has been used to predict the elastic moduli of polymorphs of sulphathiazole and carbamazepine (9). The predicted values agreed well with the experimental values after correcting for the preferred orientation of the crystals during compaction. However, neither of these studies thoroughly compared the tableting perfomance of polymorphs and the role of crystal structure on the different tableting behavior.

This work aims to compare in some depth the tableting performance of two polymorphs of sulfamerazine (SMZ). Molecular simulation enabled the different tableting properties of the two polymorphs to be related to their crystal structures.

SMZ is a commonly used antibacterial agent. Two polymorphs of SMZ have been identified and characterized (10). The Gibbs free energies, solubilities, and stabilities of the two polymorphs are very similar (11,12). These two polymorphs are enantiotropically related, such that polymorph **II** is stable at ambient temperature while polymorph **I** is stable at higher temperatures (11,12).

MATERIALS AND METHODS

Materials

SMZ was purchased as a powder from Sigma Chemical Co. (St. Louis, MO) and consisted of polymorph **I**. To crystallize disordered regions on the surfaces of the crystals, polymorph **I** (250 g) was suspended for 3 days in methanol (1200 ml, Fisher Chemical, Fair Lawn, NJ) in a 2.0 L Erlenmeyer flask. This suspension was stirred by a three-blade stirrer driven by a motor (Heidolph, model RZR-2000, Wiarton, Ontario. Canada) at 231 rpm. The flask was wrapped in aluminum foil to exclude light. The suspension was filtered by suction through a funnel at the end of the process. The final powder thus obtained was polymorph **I**, phase-pure to X-rays. Two batches of bulk powders of polymorph **II** were prepared by a similar procedure in which 250 g of raw material (polymorph **I**) were suspended for 2 weeks with 1 g of seed crystals of polymorph **II** in 1.2 L acetonitrile (11,12). For one batch, **II(A)**, a magnetic stirring bar was rotated at the bottom of the flask to facilitate stirring. For the other batch, **II(B)**, only a

[1] Department of Pharmaceutics, University of Minnesota, Weaver-Densford Hall, 308 Harvard Street S.E., Minneapolis, Minnesota 55455-0343, USA

[2] Current address: Pharmacia Corporation, 7207-259-277, 7000 Portage Rd, Portage, Michigan 49001.

[3] To whom correspondence should be addressed. (e-mail: grant001@tc.umn.edu)

0724-8741/01/0300-0274$19.50/0

three-blade stirrer was used. This longer period ensures complete conversion of the suspended powder of **I** into **II**. As a result, both **II(A)** and **II(B)** were X-ray phase-pure forms of polymorph **II**. Microscopic observations (Fig. 1) indicate that the particles in **II(A)**, 1–15 μm, are much smaller than those in **II(B)**, 10–40 μm. All solvents used in this study were of HPLC grade. All powders were stored in brown bottles over anhydrous calcium sulfate (Drierite, W.A. Hammond Drierite Company, Xenia, OH) prior to powder characterization and compaction.

Crystal Structures and Molecular Modeling

The crystal structures of two polymorphs of SMZ, **I** (reference code: SLFNMA02) and **II** (reference code: SLFNMA01) were downloaded from the Cambridge Structural Database, using the Graphic QUEST3D Software (Cambridge Crystallographic Data Center, 1995) (10,13).

From the single crystal data, the lattice structures of crystals of **I** and **II** were visualized in three dimensions using commercial software (Cerius^2 3.5, Biosym/Molecular Simulations, San Diego, CA). The theoretical powder X-ray diffraction (PXRD) patterns of **I** and **II** were calculated using the Property Prediction Module of Cerius^2.

Transmission Light Microscopy

A computer-video-enhanced microscope (Nikon Optiphoto-Pol microscope, Tokyo, Japan) equipped with imaging software (Metamorph, Universal Imaging Co., West Chester, PA) was used to characterize the powders. Microscopic observations were performed on samples immersed in silicone oil (Aldrich Chemical Company, Milwaukee, WI) using a transmitted light source.

Preparation of Tablets

Powders of suitable weigh were compressed at various compaction pressures in a split die, which allowed uniaxial compression and triaxial decompression, under a hydraulic press (Carver, model C, Menomonee, WI) to make square-faced tablets of dimension 19 mm ×19 mm × 9 mm. The punches and die were lubricated with a 5% (w/v) suspension of magnesium stearate in ethanol before each compaction and were dried. The compaction pressure ranged from 3.45 MPa to 55.2 MPa and the dwell time was 1 min. All tablets were stored over phosphorus pentoxide (0% RH) for six days before subsequent experiments. The true density, ρ_t, of the crystals was determined in triplicate by a helium pycnometer (Micromeritics, Norcross, GA) (Table 1). The tapped density of the three powders (Table 1) was determined by dropping a 20 mL graduated cylinder containing each powder of known weight 100 times from 1.5 cm height onto the bench. The dimensions of the tablets were measured to ± 0.02 mm using a dial caliper (Mitutoyo Manufacturing Co., Japan). Hence, the volume of each compact was calculated. The porosities of tablets were calculated from the true density of the powder, the weight, and the volume of the tablets.

Measurement of Tensile Strength

Tensile strength was determined in triplicate using a compressive test procedure (14). The tablet was placed between a pair of platens of width 7.8 mm, about 0.4 times the width of the square-faced tablet. The platens were padded with four layers of filter paper fixed by four layers of double-sided adhesive tape to ensure good contact and to reduce shearing stress at the edges. A transverse load was applied to the tablets at a rate of 1.6 mm/min. In this study, all the tablets split into two halves with the fracture plane running through the center of the tablets along the loading axis, indicating ideal tensile failure (14). Under these conditions, the failure tensile strength is 0.16 times the mean compressive stress (14). The tensile strength, σ, was calculated by equation (1):

$$\sigma = 0.16\, F/((7.8/1000) \cdot W) \qquad (1)$$

where F is the force at fracture and W is the thickness of the tablet. The factor, $F/((7.8/1000)\cdot W)$, represents the mean compressive stress at tensile failure. Powders consisting of various proportions of **I** and **II(A)** were prepared by geometric mixing of the polymorphic powders. Single tablets were prepared by compressing each powder mixture at 41.4 MPa for 1 min. Lubrication of the punches and die, the storage conditions, and the tensile strength determination were carried out as described for the pure powders. The porosity of each tablet was calculated from the weight percentage of each polymorph, the true density of the polymorphs (Table I), the weight of the tablet, and the volume of the tablet.

X-Ray Diffractometry

Powder X-ray diffraction (PXRD) patterns of compacts or powders were collected using an X-ray diffractometer (Siemens, model D5005, Germany) with Cu Kα radiation generated at 40 mA and 45 kV. Counts were measured using a scintillation counter. Each powder was packed into a sample

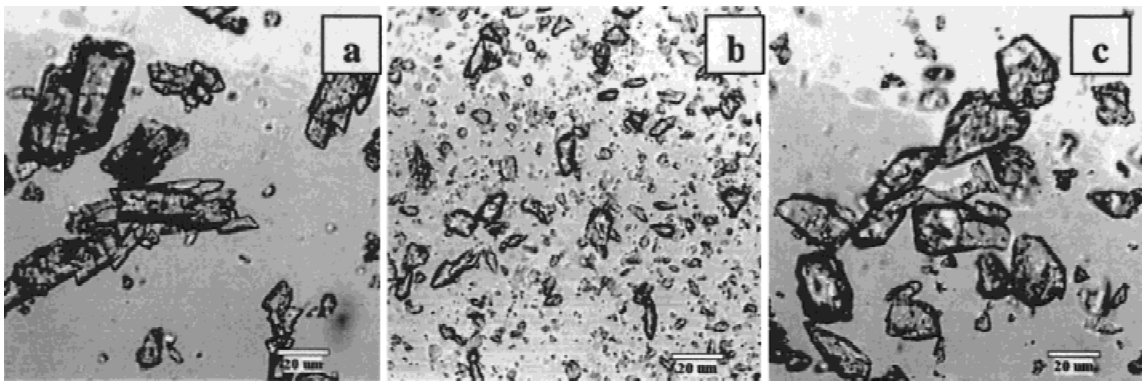

Fig. 1. Photomicrographs of three sulfamerazine powders: (a) **I**; (b) **II(A)**; (c) **II(B).**

Table I. Densities and Mechanical Properties of Three Sulfamerazine Powders (Standard Deviations in Parentheses)

Powder form	Particle size (μm)	True density[a] (g/cm^3) (n = 3)	Tapped density (g/cm^3) (n = 3)	σ_0 (MPa)[b] (n = 3)	P_y (MPa)[c] (n = 3)
I	10–40	1.335 (0.004)	0.633 (0.004)	5.10	68.4 (1.5)
II(A)	1–15	1.415 (0.005)	0.683 (0.008)	5.77	77.5 (4.5)
II(B)	10–40	1.414 (0.003)	0.751 (0.003)	3.93	86.2 (5.6)

[a] True density is measured using helium pycnometry.
[b] σ_0 is tensile strength extrapolated to zero porosity in Eq. (3).
[c] P_y is the mean yield pressure, which is derived from Heckel analysis, Eq. (2).

holder and was pressed by a clean glass slide to ensure coplanarity of the powder surface with the surface of the holder. To determine its PXRD pattern, a square-faced tablet was mounted on a small piece of modeling clay, placed at the bottom of a deeper holder, and was gently pressed down, using a flat glass slide, until the surface of the tablet was coplanar with the surface of the holder. The scans were run from 5° to 35° 2Θ, increasing at a step size of 0.05° with a counting time of 1 s for each step. To identify solid phases, the experimental PXRD patterns were compared with theoretical patterns calculated from crystal structure of **I** and **II**.

Heckel Analysis

Densification data of both polymorphs were analyzed using the Heckel equation (15,16), thus:

$$-\ln(1 - D) = KP + A \quad (2)$$

where P is the compaction pressure, D is the relative density, ρ_c / ρ_t, of the compact, K is the slope of the linear portion of the Heckel plot, and A is the intercept of the linear portion when P is zero. The reciprocal of K, termed the mean yield pressure, P_y, provides a quantitative measure of the plasticity of the material (17). A lower P_y indicates greater plasticity of a powder.

RESULTS AND DISCUSSION

Definition of Terms

To present and to discuss the results more clearly, three terms, e.g., tabletability, compressibility, and compactibility, have been defined (18) and are summarized in the following paragraphs.

Tabletability is the capacity of a powdered material to be transformed into a tablet of specified strength under the effect of compaction pressure (18). Tabletability describes the effectiveness of the applied pressure in increasing the tensile strength of the tablet and demonstrates the relationship between the cause, the compaction pressure, and the effect, the strength of the compact.

Compressibility is the ability of a material to undergo a reduction in volume as a result of an applied pressure (18). Compressibility indicates the ease with which a powder bed undergoes volume reduction under compaction pressure and is represented by a plot showing the reduction of tablet porosity with increasing compaction pressure.

Compactibility is the ability of a material to produce tablets with sufficient strength under the effect of densification (18). Compactibility shows the tensile strength of tablets normalized by tablet porosity. In many cases, the tensile strength of a tablet decreases exponentially with increasing porosity (19). In this study, we have found that equation (3) describes the compactibility of the three powders very well, thus:

$$\sigma = \sigma_0 e^{-a\varepsilon} \quad (3)$$

where σ is tensile strength, ε is porosity, and σ_0 is tensile strength extrapolated to zero porosity.

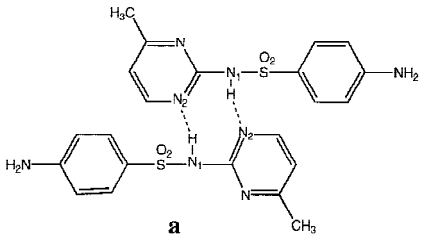

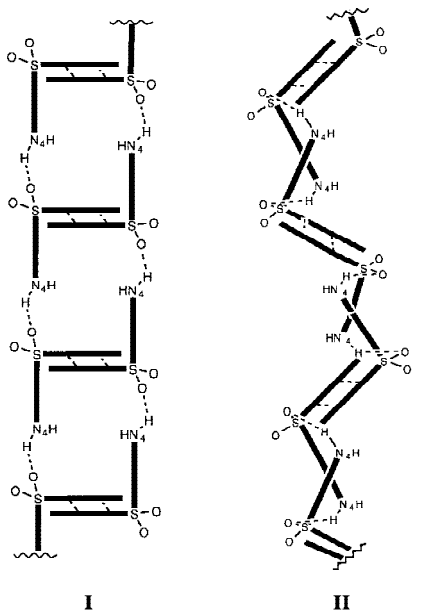

b

Scheme 1. (a) Structure of the dimer in crystals of sulfamerazine. (b) Infinite hydrogen-bond structure within sulfamerazine polymorphs: **I** and **II**. Hydrogen-bonds are indicated by broken lines. Even though the hydrogen bond connectivity patterns are the same for both polymorphs, the secondary structures are different. For clarity, only atoms directly involved in the formation of infinite chains of hydrogen bonds are shown.

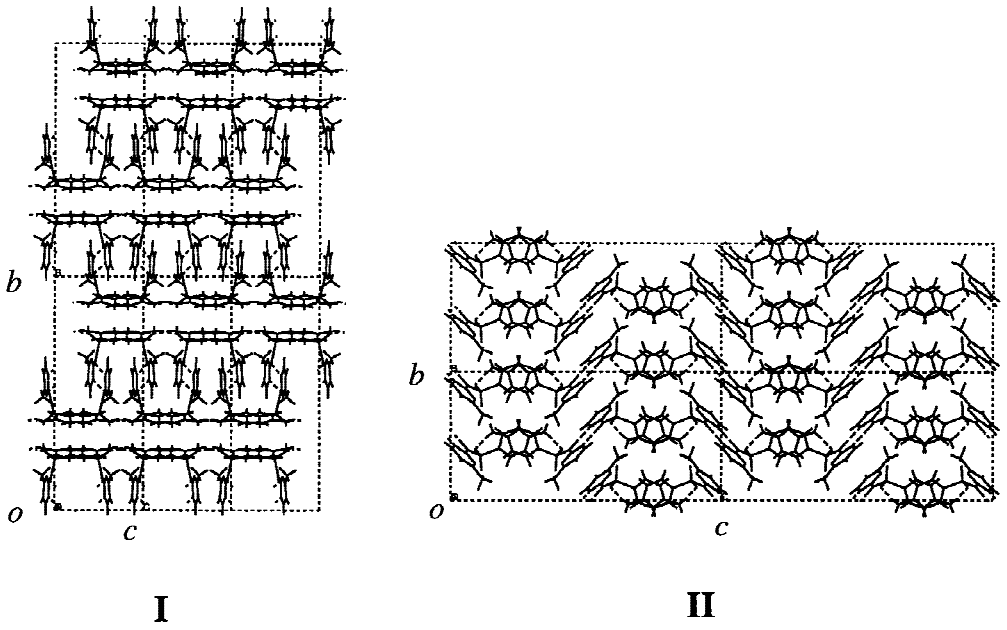

Fig. 2. The crystal structures of sulfamerazine polymorphs looking into the *a* axis: left, polymorph **I**, in which the slip planes are parallel to the *ac* plane of the unit cell; right, polymorph **II**, in which no slip plane is observed. The hydrogen bonds are indicated by dotted lines between molecules, as shown in Scheme 1b.

Crystal Structures of Two Polymorphs

The two polymorphs have the same hydrogen bond connectivity patterns but different secondary structures (10,13). In both crystals, a Z-shaped dimer (Scheme 1a) bound by two hydrogen bonds ($N_2\cdots H\text{-}N_1$) is the basic structural unit in both crystals. This dimer is pseudocentrosymmetric in **I** (10) and centrosymmetric in **II** (13). Each of the two N_4 atoms in a dimer is bound to one other dimer by a hydrogen bond ($O_1\cdots H\text{-}N_4$) forming an infinite hydrogen-bonded chain in each polymorph (Scheme 1b). These hydrogen-bonded chains are parallel to each other, while neighboring chains are displaced by a small distance along the chain direction to achieve intimate spatial arrangements. The spaces within a chain are occupied by molecules within other chains. Therefore, for steric reasons, one-dimensional hydrogen bonded chains achieve a rigid two-dimensional layered structure within the crystals. These layers lie parallel to the *ac* plane in crystals of both polymorphs (Fig. 2). No hydrogen bonding exists between these layers. Therefore, the weak van der Waals force is the main interaction between neighboring layers.

Different secondary structures of the infinite hydrogen-bonded chain give rise of the different geometries of the two-dimensional layers within crystals of **I** and **II**. Hydrogen-bonded layers within crystals of **I** are flat and can slide over their neighbors, which confers great plasticity on **I** crystals (Fig. 2). However, hydrogen-bonded layers within crystals of **II** are zigzag-shaped (Fig. 2). Because the layers interlock, slip between layers occurs with much greater difficulty within **II** crystals. Consequently, crystals of **II** exhibit low plasticity. This difference in plasticity between the different crystal structures explains the markedly different tableting behavior of these two polymorphs.

Tabletability of Polymorphs

The tabletability of the three powders follows the order: **I** >> **II(A)** > **II(B)** (Fig. 3). At the same compaction pressure, **I** always forms much stronger tablets than **II(A)** or **II(B)**. Tablets of **II(A)** are slightly stronger than those of **II(B)**. The tabletability curves of all three powders appear linear at compaction pressures less than 30 MPa. However, the curves gradually level off at higher pressures (Fig. 3). This behavior will be discussed in detail elsewhere. Briefly, tablet tensile strength increases linearly with increasing compaction pressure in the low pressure region where elastic recovery of the tablet after compression is negligible. However, at higher compaction pressures, the porosity of the tablet is already reduced substantially. Further increase of pressure causes elastic deformation of the particles rather than a decrease of pore volume in the tablet. Subsequently, tablets undergo significant elastic recovery after compression which weakens the interparticulate bonding in the tablets. Consequently, the tabletability curve levels off gradually or even decreases with increasing pressure. Tabletability describes the relationship

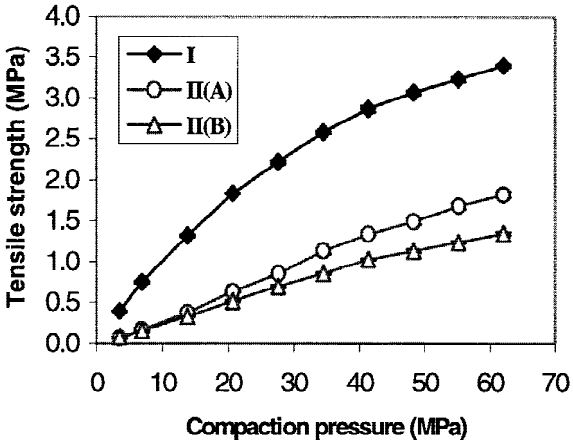

Fig. 3. Plots of tensile strength against compaction pressure, showing the tabletability of three powders of sulfamerazine, **I**, **II(A)**, and **II(B)**. The tabletability follows the order: **I** >> **II(A)** > **II(B)**.

between compaction pressure and tablet strength, but does not provide a fundamental understanding of the relationship, because tablet strength is determined by bonding area and bonding strength per unit bonding area. Contributions from each of these factors can not be separated by means of the tabletability plot alone. Therefore, even though practically useful, tabletability alone does not adequately describe the tableting performance. We therefore evaluate the compressibility and compactibility of the three powders in order to understand their differences in tableting behavior.

Tablets of the three powders, compressed at different pressures, were analyzed by PXRD. No changes in the X-ray diffraction patterns that might suggest a detectable phase transition were observed.

Compressibility of Polymorphs

The compressibility of the three powders follows the order: **I** >> **II(B)** > **II(A)** (Fig. 4). At the same compaction pressure, the porosity of the tablets follows the reverse order: **I** << **II(B)** <**II(A)** (Fig. 4). Lower porosity of a tablet corresponds to a larger interparticulate bonding area within a tablet. Therefore, the greater tabletability of **I** might be a result of its greater compressibility, which itself indicates that **I** crystals might have greater plasticity, in agreement with the fact that slip planes exist in **I** crystals but not in **II** crystals (Fig. 2). Because of their greater plasticity, crystals of **I** undergo greater plastic deformation under the same compaction pressure. Consequently, the porosity of the tablet is lower and the interparticulate bonding area is greater within tablets of **I**.

The bonding strength per unit area of different batches of the same solid phase, **II(A)** and **II(B)**, is expected to be similar. Therefore, interparticulate bonding area is the main factor that accounts for the differences in tensile strength between tablets of these two powders. The lower compressibility of **II(A)**, i.e., greater porosity at the same pressure, disfavors the strength of its tablets. If porosity is the only factor that determines the total interparticulate bonding area, we might expect a lower tabletability of **II(A)** than **II(B)**. However, this supposition is ruled out by the higher tabletability of **II(A)** (Fig. 3).

Transmission light microscopy reveals that particles of **II(A)** are smaller than those of **II(B)** (Fig. 1), presumably because of the extra attrition that may arise from the magnetic stirring bar. This observation explains the greater compressibility of **II(B)** than that of **II(A)**, because larger particles pack more effectively, as shown by the greater tapped density of **II(B)** powder (Table 1). However, smaller particles often have more points of contact between neighboring particles at the same porosity, which favors stronger tablets. In this case, the favorable effects of more numerous points of contact of **II(A)** on tablet strength overcome the unfavorable effects of the greater porosity of **II(A)** tablets. Consequently, the tabletability of **II(A)** is greater than that of **II(B)**.

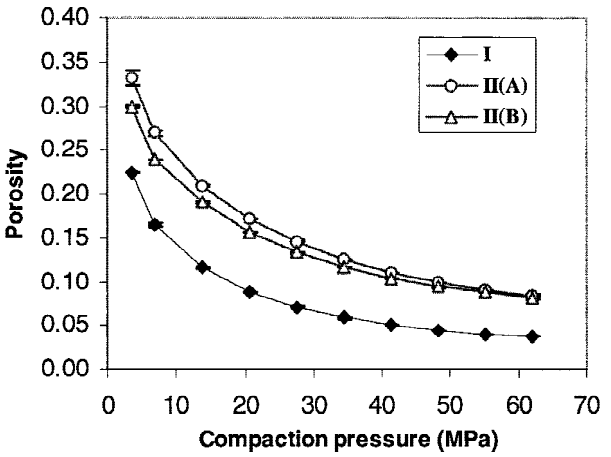

Fig. 4. Plots of tablet porosity against compaction pressure, showing the compressibility of three powders of sulfamerazine, **I**, **II(A)**, and **II(B)**. The compressibility follows the order: **I** >> **II(B)** > **II(A)**.

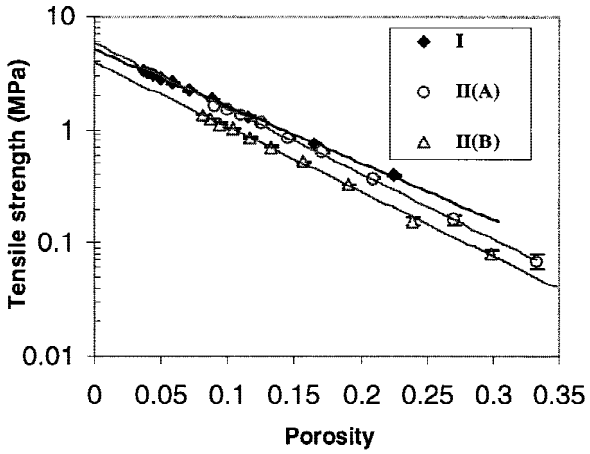

Fig. 5. Plots of tensile strength against tablet porosity, showing the compactibility of three powders of sulfamerazine, **I**, **II(A)**, and **II(B)**. The compactibility follows the order: **II(B)** <**II(A)** ≈ **I**.

Compactibility of Polymorphs

Compactibility normalizes tablet strength by porosity. For all three powders, the tensile strength decreases exponentially with increasing porosity (Fig. 5). However, although **I** exhibits much greater tabletability, its compactibility is not much greater than that of **II(A)** (Fig. 5). This result agrees with the earlier conclusion that the greater compressibility of **I,** which is a result of the slip planes in its crystals, is the origin of the greater tabletability of **I**. Therefore, the superior tabletability of **I** is a result of its greater interparticulate bonding area and not of its greater bonding strength per unit bonding area.

Figure 5 also indicates that the compactibility of **II(B)** is significantly lower than that of **II(A)**. This result arises from the larger size of crystals in **II(B)** which lowers both the porosity and tensile strength of tablets at the same compaction pressure. Therefore, on a compactibility plot, data points of **II(B)** move towards lower values on both the tensile strength axis and porosity axes, when compared with data points of **II(A)** at the same compaction pressure. Therefore, the compactibility of **II(B)** is significantly lower than that of **II(A)**. Consequently, the tensile strength of **II(B)** extrapolated to zero porosity, σ_0, is significantly lower than that of **II(A)** (Table 1).

Because of its great influence on compactibility, particle size must be well controlled, especially when comparing tableting behavior of two different materials. Ideally, powders of a series of different sizes should be studied for each mate-

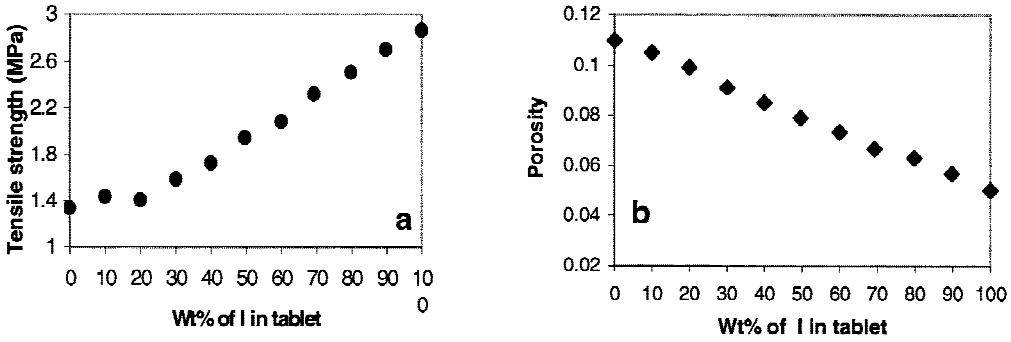

Fig. 6. (a) Tensile strength and (b) porosity of tablets prepared from powder mixtures of two polymorphs, **I** and **II(A)**, of sulfamerazine compacted at a pressure of 41.4 MPa.

rial before meaningful conclusions can be drawn. Without proper control of particle size, values of σ_0 of different materials may not correlate well with their lattice energy, even though some studies have successfully correlated σ_0 with the cohesive energy of powders (20).

Heckel Analysis

The mean yield pressure, P_y, of three powders was calculated from Heckel plots and are summarized in Table 1. The P_y of the three powders follows the order: **I** < **II(A)** < **II(B)**. P_y of **I** is significantly lower than that of **II(A)** and **II(B)**, corresponding to the greater plasticity of **I**. P_y of **II(A)** is lower than that of **II(B)**, i.e., smaller particles correspond to lower mean yield pressure. This relationship between mean yield pressure and particle size agrees with other observations (21). In explanation, the pores in the tablets prepared from larger crystals are larger than those from smaller crystals. Therefore, the reduction of the pore volume by plastic deformation of crystals is less efficient for larger crystals. Consequently, the volume reduction of larger crystals is lower and tablets compacted from larger crystals is more porous than tablets from smaller crystals under the same pressure. Therefore, ln ε increases more slowly with increasing pressure for larger crystals. Consequently, the linear portion of the Heckel plot has a lower slope and therefore the mean yield pressure calculated from equation (2) is greater for larger crystals. On the other hand, the difference in P_y between **II(A)** and **II(B)** reflects the different compressibilities of the two powders (Fig. 4).

Influence of Polymorphic Content on Tableting Performance

When compressed at the same pressure, 41.4 MPa, tablet tensile strength increases progressively with increasing proportions of **I** in mixtures with **II(A)** (Fig. 6a). The increase in tensile strength corresponds to a decrease in porosity of the tablets (Fig. 6b). Lower porosity increases the interparticulate bonding area, leading to stronger tablets. This result further confirms that the greater tabletability of **I** crystals arises from the greater plasticity which their slip planes confer and which leads to more extensive plastic deformation and larger interparticulate bonding area in the tablets.

CONCLUSIONS

Slip planes provide **I** crystals greater plasticity and therefore greater compressibility and tabletability over **II**. This study indicates that it is possible to predict the tableting performance of different polymorphs of a drug, provided that their crystal structures are available. The polymorphs whose crystals have slip planes is expected to have superior tableting performance than those without them. For the same polymorph, larger crystals lead to slightly lower tabletability and slightly better compressibility and therefore significantly lower compactibility. When the proportion of **I** increases in a powder mixture containing both polymorphs, **I** and **II**, the tablet tensile strength increases in accordance with the decreasing tablet porosity.

Tabletability alone is inadequate to characterize the relative tableting behavior of pharmaceutical powders. Comprehensive understanding can only be achieved by simultaneously considering compressibility, compactibility, crystal structure, and particle size.

ACKNOWLEDGMENTS

We thank the American Foundation for Pharmaceutical Education for awarding a Pre-Doctoral Fellowship to C. Sun. We also thank the Supercomputing Institute of the University of Minnesota for financially supporting our use of the Medicinal Chemistry / Supercomputing Institute Visualization – Workstation Laboratory.

REFERENCES

1. D. J. W. Grant. Theory and origin of polymorphism, In H. G. Brittain (ed.), *Polymorphism in Pharmaceutical Solids,* Marcel Dekker, Inc., New York, NY, 1999 pp. 1–34.
2. U. Conte, P. Colombo, C. Caramella, G. P. Bettinetti, F. Giordano, and A. La Manna. On the direct compression of sulfamethoxydiazine (SMD) polymorphic forms—I. *Il Farmaco (Ed. Pr.)* **30**:194–206 (1974).
3. M. Otsuka, H. Hasegawa, and Y. Matsuda. Effect of polymorphic transformation during the extrusion-granulation process on the pharmaceutical properties of carbamazepine granules. *Chem. Pharm. Bull.* **45**:894–898 (1997).
4. M. Otsuka, T. Matsumoto, S. Higuchi, K. Otsuka, and N. Kaneniwa. Effect of compression temperature on the consolidation mechanism of chlorpropamide polymorphs. *J. Pharm. Sci.* **84**:614–618 (1995).
5. M. D. Tuladhar, J. E. Carless, and M. P. Summers. The effects of polymorphism, particle size and compression pressure on the dissolution rate of phenylbutazone tablets. *J. Pharm. Pharmacol.* **35**:269–274 (1982).
6. M. W. Y. Wong and A. G. Mitchell. Physicochemical characterization of a phase change produced during the wet granulation of chlorpromazine hydrochloride and its effects on tableting. *Int. J. Pharm.* **88**:261–273 (1992).
7. T. Yamaoka, H. Nakamachi, and K. Miyata. Studies on the char-

acteristics of carbochromen hydrochloride crystals. II. Polymorphism and cracking in the tablets. *Chem. Pharm. Bull.* **30**:3695–3700 (1982).
8. G. Nichols and C. S. Frampton. Physicochemical characterization of the orthorhombic polymorph of paracetamol crystallized from solution. *J. Pharm. Sci.* **87**:684–693 (1998).
9. R. J. Roberts, R. S. Payne, and R. C. Rowe. Mechanical property predictions for polymorphs of sulphathiazole and carbamazepine. *Eur. J. Pharm. Sci.* **9**:277–283 (2000).
10. M. R. Caira and R. Mohamed. Positive identification of two orthorhombic polymorphs of sulfamerazine (C11H12N4O2S), their thermal analyses and structural comparison. *Acta Cryst*. **B48**:492–498 (1992).
11. G. G. Z. Zhang. *Influences of Solvents on Properties, Structures, and Crystallization of Pharmaceutical Solids,* Ph.D. Thesis, University of Minnesota: Minneapolis MN, 1999, pp. 127–178
12. G. G. Z. Zhang, C. Gu, M. T. Zell, R. T. Burkhardt, and D. J. W. Grant. Crystallization and transformation of sulfamerazine polymorphs. *J. Pharm. Sci.* Submitted (2001).
13. K. R. Acharya, K. N. Kuchela, and G. Kartha. Crystal structure of sulfamerazine. *J. Crystallogr. Spectrosc. Res.* **12**:369–376 (1982).
14. E. N. Hiestand and C. B. Peot. Tensile strength of compressed powders and an example of incompatibility as end-point on shear yield locus. *J. Pharm. Sci.* **63**:605–612 (1974).
15. R. W. Heckel. Density-pressure relationships in powder compaction. *Trans. Metall. Soc. AIME* **221**:671–675 (1961).
16. R. W. Heckel. An analysis of powder compaction phenomena. *Trans. Metall. Soc. AIME* **221**:1001–1008 (1961).
17. J. A. Hersey and J. Rees. Deformation of particles during briquetting. *Nature (Phys. Sci.)* **230**:96 (1971).
18. E. Joiris, P. D. Martino, C. Berneron, A.-M. Guyot-Hermann, and J.-C. Guyot. Compression behavior of orthorhombic paracetamol. *Pharm. Res.* **15**:1122–1130 (1998).
19. E. Ryshkewitch. Compression strength of porous sintered alumina and ziroconia. *J. Am. Cer. Soc.* **36**:65–68 (1953).
20. R. J. Roberts, R. C. Rowe, and P. York. The relationship between the fracture properties, tensile strength and critical stress intensity factor of organic solids and their molecular structure. *Int. J. Pharm*. **125**:157–162 (1995).
21. P. York. Particle slippage and rearrangement during compression of pharmaceutical powders. *J. Pharm. Pharmacol.* **30**:6–10 (1978).